KSTLE International Journal, Vol. 2, No. 2, December 2001, pp. 85-92

The Influence of Contact Shape on the Slip Regime in Contact-induced Failure

Hyung-Kyu Kim†, Heung-Seok Kang and Kee-Nam Song

Korea Atomic Energy Research Institute, 150 Dukjin-dong, Yusong-ku, Taejon 305-353, Korea

Abstract : The variation of contact traction induced by different contact shapes is studied experimentally and theoretically. Considerations for the contact shape are rounded, truncated and truncated with rounding punches. A fretting wear experiment is conducted with the contact configuration of the strip on the tube specimens. The strip specimen is pressed to form the end profile of a rounded and truncated with rounding punches shape. Wear on the tube is investigated, which is regarded as the slip region of the contact surface. Taken into consideration is the general solution of the normal traction in the case of the indentation by a punch with its end profile of the combination of parabolas. Then, partial slip solution is obtained numerically, which is compared with the wear on the tube. The radius of the rounding and the obliquity of the edge truncation affect the tractions considerably. It is found that the proper choice of the end profile can restrain the contact-induced failure such aswear.

Keywords : Contact shape, truncated and rounded punch, contact traction, partial slip

Introduction

In the contacting components of mechanical structures, it is widely found that failure occurs on the contact during service. The mode of it is, in general, wear on the contact surface and/or fatigue cracking in the contacting bodies. Wear loosens fittings and joints of mechanical components which can cause the degradation of load transfer and sealing performance. The growth rate of a crack initiated from the contact edge (usually termed as a fretting fatigue crack) is often much higher than that of a normal fatigue crack. Premature failure has been reported due to the fretting fatigue cracking [1-2]. In short, contact-induced failure reduces the expected design life considerably. So, it is important to know the mechanism of such failure to improve the life.

One of the approaches on the mechanism is to analyze the stresses of contacting bodies. From the mechanical design viewpoint, the stress-based criteria are widely used (e.g., Von Mises or Tresca yield criterion). The internal stress of the contacting bodies is influenced directly by the contact traction, which is affected by the geometry of contact shape, i.e. the end profile of the contacting body. Square punch, wedge and cylinder are often referred to as the basic shapes of the end profile. The normal contact tractions of those conventional contact shapes have been developed well [3]. On the other hand, a special concern is necessary for the shear traction. Partial slip or gross slip condition is constituted on the contact surface according to the shear force exerted on the contacting bodies.

If the shear force is less than that which causes gross relative movement between the contacting bodies (gross slip), partial slip is constituted. The outer portion of the contact area slips relatively while the inner portion sticks when partial slip is formed. As the shear force increases, gross slip (or sliding) occurs and the whole contact area slips. If Coulombs friction law is adopted, $|q(x)| < \mu |p(x)|$ in the stick region of the partial slip regime, where μ is static friction coefficient, $p(x)$ and $q(x)$ are the normal and shear tractions, respectively. In the slip region of partial slip and in the case of gross slip as well, $|q(x)| = \mu |p(x)|$. It is important to know the slip regime since wear occurs on the slip region of the contact surface. In fact, the shear rather than the normal force on the contact plays the major role in wear [4].

As aforementioned for the normal traction, the contact shape also influences shear traction. In other words, the slip regime can be altered corresponding to the contact shape even though the same shear force is applied. If we focus on the wear damage, it may be required to maintain the partial slip as long as possible during the increase of shear force since the wear must be less than that when gross slip occurs.

In this study, three different contact shapes are considered to investigate their influence on the contact-induced failure, especially wear. Experiments are carried out with the indenter of rounded and truncated punches, which are in contact with a tube to consider the different contact shapes. Contact mechanical analysis is carried out to study the influence of the contact shape theoretically. It tries to explain the experimental results, especially the slip region and wear, by the analysis. It is addressed that dimensioning of the end profile is important to control the contact-induced failure.

Experiment

Specimens and Experimental Condition

To investigate the influence of the contact shape, two different

†Corresponding author; Tel: 82-42-868-2111, Fax: 82-42-868-0565
E-mail: hkkim1@nanum.kaeri.re.kr

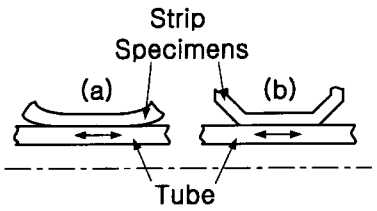

Fig. 1. Two different contact shapes in the experiment: (a) rounded punch and (b) truncated punch.

types of indenter are designed such as rounded and truncated punches schematically shown in Fig. 1. These specimens were fabricated by pressing a strip of 0.46 mm thickness. The substrate specimen is a tube of which the thickness is 0.6 mm and the outer diameter is 9.5 mm. The specimens are designed for the fuel rod (tube specimen) and the spacer grid (strip specimen) of light water reactor nuclear fuel, so the material used is Zircaloy-4 whose properties are given in Table 1.

As shown in Fig. 1, the two contacting specimens (i.e., tube and strip) are aligned along the longitudinal direction. A line contact is approximated with this configuration, which the two-dimensional schematic of Fig. 1 is attributed to. Before the experiments, both tube and strip specimens are cleaned with acetone in the ultrasonic cleaning bath. During the experiment, the tube oscillates longitudinally with contacting normal force of 10, 30 and 50 N. The relative slip displacement (range) is varied as 10, 30, 50, 80, 100, 150 and 200 μm for each normal force. The frequency of oscillation is set at 30 Hz. The experiment is conducted in air at room temperature. Wear scar on the tube specimen is observed using an optical microscope when the number of oscillation cycles reaches 100,000.

After each experiment, wear depth of the tube is measured from the wear contour logged by a surface roughness tester. Wear volume is evaluated from the whole contours which covers the wear scar on the tube using a specially developed program [5]. Fig. 2 shows the schematic diagram of the fretting wear tester used for the present experiment. Detailed explanation of the tester can be seen in [6], so it is not re-written here.

Results

Partial and gross slip can be distinguished from the wear scar on the tube observed from the microscope. Typical wear views are given in Figs. 3 through 6 for each shape of the punch and slip regime. As is accepted in general, partial slip is found to

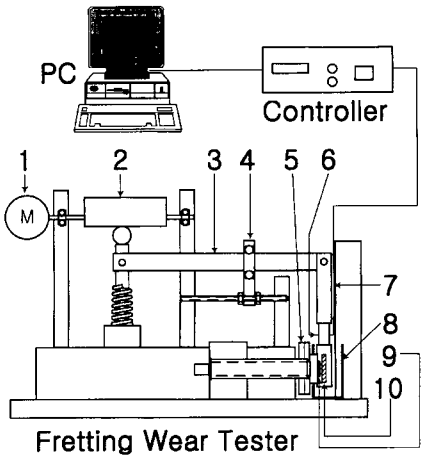

Fig. 2. Schematic diagram of the fretting wear tester used in the experiment.

occur when the normal force increases and the slip displacement decreases. In the present experiment, the transition from partial to gross slip appears at 50 μm when the normal force is 30 N. When the normal force is 10 and 50 N, partial slip prevails until the slip displacement is 30 and 80 μm, respectively.

A surface roughness tester gives wear contour in the direction of tube thickness. Figs. 3 through 6 also show the results of the contours in the case of partial and gross slip regimes. Since the contact surface is worn out if wear occurs, it appears in the negative region of the plots. The length of wear can be readily estimated if the wear scar and the contour are compared in each plot. Although the contours are very much irregular, the overall shape of them can be approximated as a "W" in shape. In partial slip regime, it is generally known that the wear contour has a "W" shape since the slip (wear) region locates in the vicinity of the contact edges, and there is no slip in the central region of the contact. The wear of partial slip regime is more distinctively found when the truncated punch specimen is used.

In the case of gross slip, it has often been reported that the wear contour had a "V" or "U" shape, which implied that the central region wears out severely. However, in the present experiment, the contour has a "W" shape still in gross slip. This is more apparent in Fig. 6, which shows the gross slip by truncated punch specimen. Actually, it is expected from the view of the wear scar on the tube. The central part of the scar is

Table 1. Mechanical and chemical properties of Zircaloy-4.

Mechanical properties (at room temperature)				
Tensile strength	Yield strength (0.2% offset)	Elongation in 2″	Elastic Modulus	Poisson's Ratio
470 MPa	315 MPa	31%	136.6 GPa	0.294

Chemical composition (wt. %)						
Sn	Fe	Cr	O	C	Si	Zr
1.28	0.22	0.12	0.114	0.013	0.010	remained

(a) Wear view by microscope (X 50)

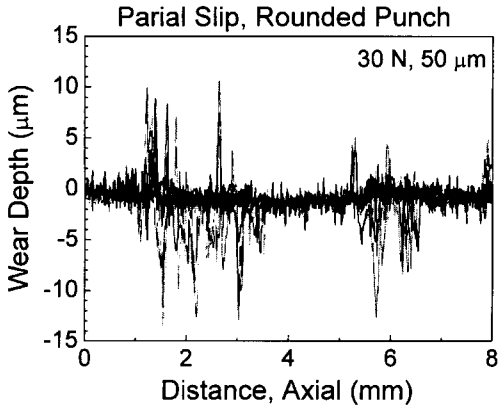

(b) Wear scar by roughness tester

Fig. 3. Wear view and scar by rounded punch specimen in the case of partial slip.

(a) Wear view by microscope (X 50)

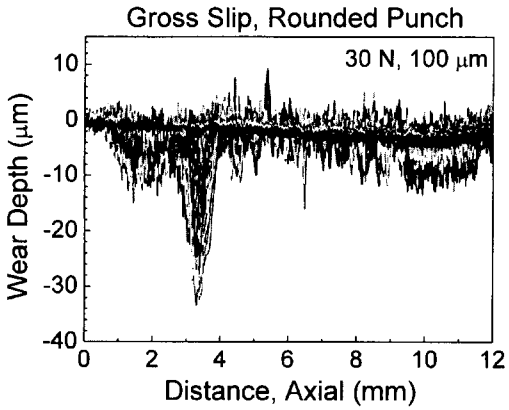

(b) Wear scar by roughness tester

Fig. 4. Wear view and scar by rounded punch specimen in the case of gross slip.

much narrower than that at both edges. The "W" and "U" shaped contours in gross slip have been discussed elsewhere [7], where a ball on a flat was the contact configuration. In this regard, it may cause considerable error if wear volume is approximated by assuming it as a simple geometry (e.g., hemisphere of semi ellipse). Resultantly, it is regarded that the contact shape also affects the wear contour.

The slip regime with respect to the normal force and the slip displacement can be drawn as a so-called "fretting map". Fig. 7 shows the overlapped view of the present result onto the previous presentation of the fretting map [8]. The abscissa represents the amplitude of the slip displacement, so the slip range used in the present experiment is twice the value of it. It can be seen that the area of partial slip regime by the present experimental result is larger than that of previous research [8].

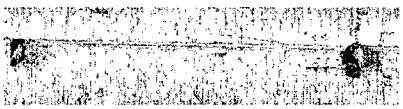

(a) Wear view by microscope (X 50)

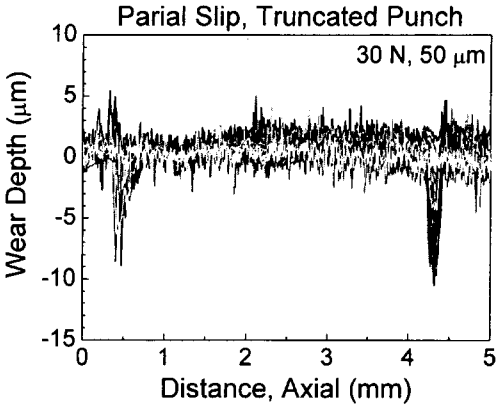

(b) Wear scar by roughness tester

Fig. 5. Wear view and scar by truncated punch specimen in the case of partial slip.

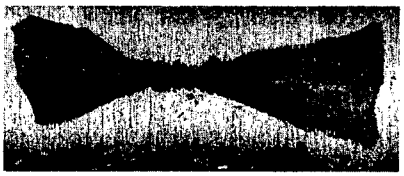

(a) Wear view by microscope (X 50)

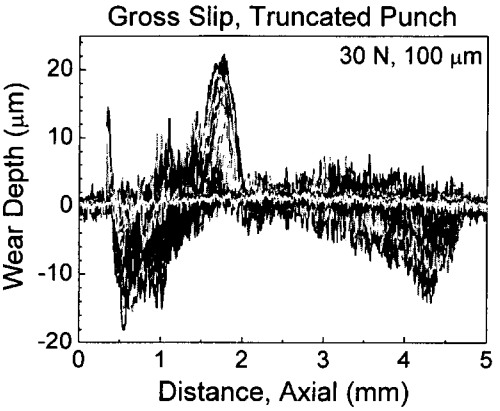

(b) Wear scar by roughness tester

Fig. 6. Wear view and scar by truncated punch specimen in the case of gross slip.

The previous experiment [8] was conducted with a ball on a flat configuration. Therefore, it can be said that the fretting map needs to be re-evaluated depending on the contact shape.

The wear volume is calculated to be 28.84×10^3, 634.19×10^3, 39.23×10^3 and $1760.5\ 6\times 10^3$ μm^3 for Figs. 3, 4, 5 and 6, respectively. It is seen that the volume increases by a factor of more than 20 from partial to gross slip for the rounded punch specimen. It is more than 40 for the truncated one. Considerable volume increase is found when gross slip occurs. However, the increase rate is always greater in the case

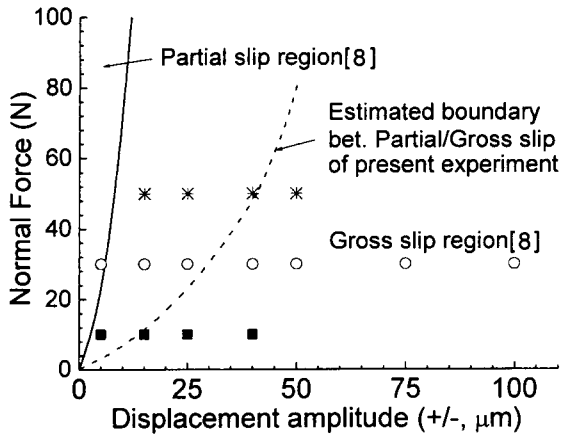

Fig. 7. The estimated boundary between partial and gross slip in the present experiment.

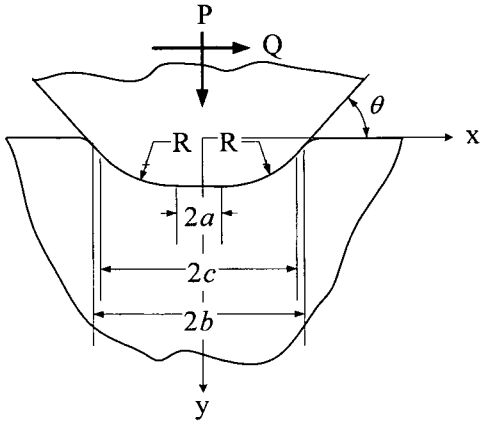

Fig. 8. Contact configuration of present analysis.

of the truncated punch specimen. Wear region is longer in the case of the rounded punch specimen. However, the wear volume is found to be greater in the case of the truncated punch specimen than in the rounded one. This is due to the difference in contact width. In the direction perpendicular to the tube length, the truncated punch specimen has a concave contour, while the rounded one has a convex contour. So, it is expected that the contact width by the truncated is larger than that by the rounded. Although there is width effect on wear volume, it is certain that there occurs considerable volume increase from partial to gross slip for each contact shape. From these experimental results, it is necessary to consider the influence of the end profile of the contacting bodies (referred to as "contact shape" presently) to study the contact-induced failure including wear. To this end, contact mechanics are to be consulted, which will be presented in the next section.

Contact Mechanical Analysis

Definition of end profile

If a smooth end profile is assumed for an indenter, it is expressed by a parabolic function or a combination of parabolic functions. To accommodate the contact shape used in the experiment, the profile is defined as the combination of them. So to speak, a punch with flat region of $2a$ and edge radius of R is chosen as the basic shape (rounded punch; R-punch). Then, the radius regions are replaced by straight lines with obliquity, θ (truncated punch; T-punch). In addition to those, a corner rounding of radius R is inserted in between the flat and the oblique regions (truncated and rounded punch; TR-punch). Fig. 8 shows the most generalized shape of TR-punch. R-punch and T-punch can be readily generated by choosing the relevant regions from TR-punch. For all the cases, the contact region is defined as $2b$. In the case of TR-punch, the oblique region begins (and the rounding ends) at $x = \pm c$.

In contact mechanics, the relationship between the elastic deformation of contacting bodies and the contact traction is written as:

$$\frac{E^*}{2}\frac{dh(x)}{dx} = \frac{1}{\pi}\int_{-b}^{b}\frac{p(\eta)}{x-\eta}d\eta - \beta q(x), \tag{1}$$

$$\frac{E^*}{2}\frac{dg(x)}{dx} = \frac{1}{\pi}\int_{-b}^{b}\frac{q(\eta)}{x-\eta}d\eta + \beta p(x). \tag{2}$$

where, $p(x)$ and $q(x)$ are the normal and tangential (shear) tractions on the contact, respectively. $h(x)$ and $g(x)$ are the elastic displacements in the normal and tangential directions, respectively. E^* and β are defined as follows:

$$\frac{1}{E^*} = \frac{(1-\nu_1^2)}{E_1} + \frac{(1-\nu_2^2)}{E_2}, \tag{3}$$

$$\beta = \frac{1}{2}\left[\frac{\{(1-2\nu_1)/G_1\} - \{(1-2\nu_2)/G_2\}}{\{(1-\nu_1)/G_1\} + \{(1-\nu_2)/G_2\}}\right]. \tag{4}$$

where, the subscripts 1 and 2 designate the two contacting bodies. ν is the Poisson ratio and G is the shear modulus of the contacting material.

To solve the coupled singular integral equations of Eqs. (1) and (2), the Goodman approximation is useful and widely used [3]. That is, $p(x)$ is to be obtained at first with assuming $q(x) = 0$ temporarily. And then, $q(x)$ is to be evaluated from Eq. (2). Therefore, the equation to be started with is

$$\frac{E^*}{2}\frac{dh(x)}{dx} = \frac{1}{\pi}\int_{-b}^{b}\frac{p(\eta)}{x-\eta}d\eta. \tag{5}$$

Eq. (5) is certainly justified for the present problem since the two contacting bodies in the present experiment are made from the same material (Zircaloy-4) so that $\beta = 0$.

To obtain $p(x)$ in Eq. (5), $h(x)$ should be defined. For the present contact shapes, it can be expressed as a combination of parabolas. For instance, two oblique lines, two radii and one horizontal line constitute the end profile of TR-punch. In short, $h(x)$ of Eq. (5) is composed of $h_i(x)$s at each subdivided interval, i of the whole contact, i.e.

Table 2. $h'(x)$ for each contact shape.

Region No. (i)	Rounded Punch		Truncated Punch		Truncated & Rounded Punch	
	K_i	L_i	K_i	L_i	K_i	L_i
1	-	-	0	θ	0	θ
2	$-1/R$	$-a/R$	-	-	$-\theta/(c-a)$	$-a\theta/(c-a)$
3	0	0	0	0	0	0
4	$-1/R$	a/R	-	-	$-\theta/(c-a)$	$a\theta/(c-a)$
5	-	-	0	$-\theta$	0	$-\theta$

$$h(x) = \sum_{i=1}^{n} h_i(x) = \sum_{i=1}^{n} \left(\frac{K_i}{2} x^2 + L_i + M_i \right) \tag{6}$$

where, n is the number of subdivided regions. K_i, L_i and M_i are constants.

Now, the first derivative of $h(x)$ is

$$\frac{dh(x)}{dx} = h'(x) = \sum_{i=1}^{n} (K_i x + L_i) . \tag{7}$$

Table 2 gives the constants K_i and L_is for the present contact shapes.

General solution of the normal traction

The general solution of Eq. (5) into which Eq. (7) is plugged has been presented recently [9] such as

$$\frac{bp(\varphi)}{P} = -\frac{1}{\pi \cos\varphi} \left[1 + \frac{E^* b}{2P} I(\varphi) \right] \tag{8}$$

where, P is the normal load on the contact and $I(\varphi)$ is defined as follows.

$$I(\varphi) = \frac{b}{2} \sum_{i=1}^{n} K_i \left(\Delta\varphi_i + \frac{\Delta \sin 2\varphi_i}{2} \right) + \sum_{i=1}^{n} \{ K_i b \sin\varphi + L_i \} \times \tag{9}$$

$$\left[\Delta\cos\varphi_i - \Delta\varphi_i \sin\varphi + \cos\varphi \ln \left| \frac{\cos((\varphi + \varphi_i)/2)}{\cos((\varphi + \varphi_{i+1})/2)} \frac{\sin((\varphi - \varphi_{i+1})/2)}{\sin((\varphi - \varphi_i)/2)} \right| \right]$$

In Eq. (9), $\Delta\varphi_i \equiv \varphi_{i+1} - \varphi_i$, $\Delta\cos\varphi_i \equiv \cos\varphi_{i+1} - \cos\varphi_i$, $\Delta\sin 2\varphi_i \equiv \sin 2\varphi_{i+1} - \sin 2\varphi_i$ and $\varphi_i = x_i/b$.

Eq. (8) provides the very useful solution of normal traction since it accommodates any contact shape if it can be described as a combination of parabolas. In fact, moreover, almost all the contact shapes found in the engineering field can be described in this way.

The contact semi-width b is influenced by P, E^* and $h(x)$. It is obtained by

$$-\frac{2P}{E^* b} = \frac{b}{2} \sum_{i=1}^{n} K_i \left(\Delta\varphi_i - \frac{\Delta \sin 2\varphi_i}{2} \right) - \sum_{i=1}^{n} L_i \Delta\cos\varphi_i = 0 . \tag{10}$$

Comparison of normal tractions

Fig. 9 gives the typical results of $p(x)$ for each contact shape when $P/(E^*a) = 1.0$. For easy comparison among the shapes, the width of flat region ($2a$) was set constant for all the calculations and used as a normalization factor of the rounding radius R of R- and TR-punches. The traction in the case of R-punch is shown in Fig. 9(a) where $p(x)$ appears finite and smooth. When the corner radius increases, the traction decreases and the location of the maximum traction moves inward due to the expansion of the contact region. However, a sharp peak is found at the transition point from the flat to the oblique region in the case of T-punch (Fig. 9(b)). The location of maximum traction moves inward as the obliquity increases due to the same reason as that of R-punch (i.e., expansion of contact region).

In the case of indentation by TR-punch (Fig. 9(c)), both traction shapes are found. The corner radius between the flat and the oblique regions is set $R/a = 1.0$. If the obliquity increases, the traction is like that of R-punch, while it becomes that of T-punch as the obliquity decreases. This means that the rounding effect (i.e., traction smoothing) decreases as the obliquity decreases since the flat and the corner regions become relatively smaller compared with the whole contact region. The magnitude of the radius also affects the traction shape. This is given in Fig. 10, where the obliquity is set at 15° and the rounding radius varies. The traction becomes that of R-punch and is distributed more smoothly as the radius increases. The maximum traction increases as the radius decreases. Resultantly, both the rounding radius and the obliquity affect the traction shape induced by TR-punch. To avoid the sharp traction can be one of the methods to alleviate contact-induced failure. Therefore, it is necessary to consider the magnitude of the radius and the obliquity in designing the contacting components.

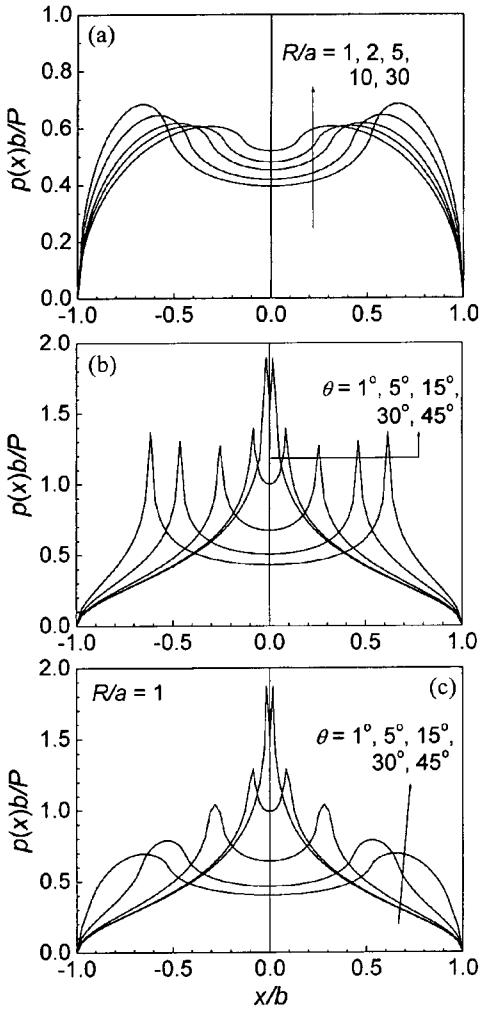

Fig. 9. Normal tractions for each contact shape with varying rounding radius and obliquity; (a) R-punch (b) T-punch and (c) TR-punch.

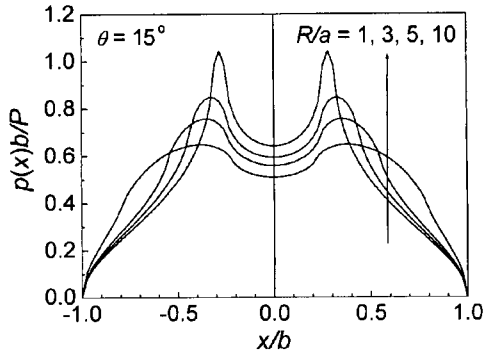

Fig. 10. Normal tractions by TR-punch with the variation of radius (when θ = 15°).

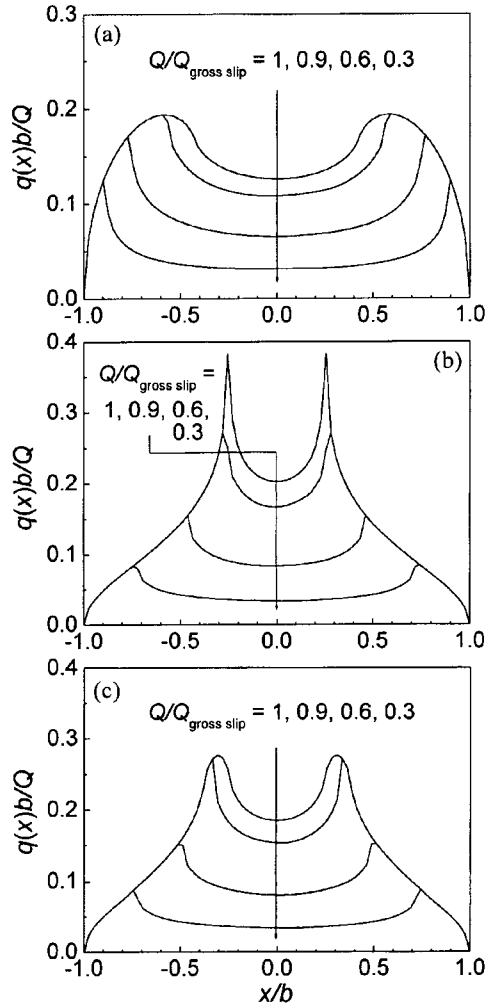

Fig. 11. Variation of shear tractions for each contact shape during the increase of shear force Q; (a) R-punch at *R/a* = 2.0 (b) T-punch at θ = 15° and (c) TR-punch at *R/a* = 2.0 and θ = 15°.

Partial slip solution

In general, contact-induced failure does not occur by normal force only. Cyclic shear is necessary to cause wear or fatigue cracking. Actually, the cyclic shear on the contact can be widely found in the mechanically contacting components during service (e.g., bolt and rivet joints, press fits and so on). Vibration is the most general source of the cyclic shear on the contact. During the cyclic shear, partial slip condition is usually constituted in the early stage of the life of the components since the tightness between the contacting components is intact. So the relative slip displacement must be small or even close to zero. As the cycle continues, the tightness is degraded due to wear evolution so that the increased slip displacement results in gross slip. When gross slip occurs, wear increases considerably as experienced in the experiment. To prolong the period of partial slip is one of the ways to restrain wear damage. Therefore, it is important to consider the partial slip condition in the mechanical design stage.

On the other hand, it is more difficult to obtain the shear traction in the case of partial slip than that of gross slip since the traction of the central stick region as well as the stick/slip boundary vary corresponding to not only the shear force but also the sequence of it [3]. The gross slip solution can be achieved without difficulty by simply multiplying the friction

coefficient to the normal traction if the Coulomb friction law is followed. So, the partial slip solution is meaningful for the contact-induced failure analysis. Analytically, the Midlin-Cattaneo solution is widely known [3], which is concerned with the one-dimensional shear of contacting cylinders. If the contact shape is not simple and/or two-dimensional shear is considered, the numerical method can give the solution efficiently [10]. In this paper, the developed numerical method [10] is used to obtain the partial slip solution.

What is brought into focus from the present analysis is the increase of slip region for R-, T- and TR-punches corresponding to the increase of shear force. Fig. 11 shows the results from each punch shape, where the shear traction of gross slip ($Q/Q_{\text{gross slip}} = 1.0$; Q is shear force) is also given. The geometrical parameters for Fig. 11 are $R/a = 2.0$ for R-punch, $\theta = 15°$ for T-punch, and $R/a = 2.0$ and $\theta = 15°$ for TR-punch. The general feature of the behaviour of the slip region is found, i.e. it starts from the contact edge and expands inward as the shear force increases.

However, what is found interesting is that the slip region cannot expand further into the central region inside the peak (maximum) tractions as long as partial slip condition prevails. It is found that gross slip occurs immediately after the shear traction reaches the maximum. It has been analytically solved, in the case of the rounded punch, that partial slip is available only when the contact boundary locates in the rounding region [11]. This means that, together with the above numerical result of present work, the maximum traction appears at the location of the transition from the central flat to the edge rounding regions. In the case of contacting cylinders (the Hertz contact), the normal traction profile is semi-ellipse. So the slip region can expand continuously to the center of contact without such an immediate jump seen in the present cases. Conclusively, the consideration of contact shape is important to control the contact-induced failure since it also influences the expansion behaviour of the slip region, which directly results in the wear region.

Discussions

The contact shapes used in the experiment can be defined as R-punch and TR-punch referred to in the analysis. The specimen of rounded punch in the experiment (Fig. 1(a)) is regarded as R-punch with large radius ($R/a > 5$). From the feature of the traction by R-punch (Fig. 9(a)), the maximum of it is not high compared with the traction by T-punch. The specimen of truncated punch (Fig. 1(b)) is regarded here as TR-punch with $\theta = 45°$ rather than T-punch. This is because the specimens are made from a strip and fabricated by pressing. Although the overall shape looks like T-punch, the corner (i.e., the starting point from the flat to the oblique regions) must have a rounding part even though the radius of it is very small. In fact, it is very difficult to manufacture the perfect shape of T-punch. Even if it is achieved, after some shear cycles, the sharp corners of the perfect T-punch can be removed easily due to the high stress and wear at the corners, which probably results in TR-punch. Referring to Figs. 9(c) and 10, it is thought that a high traction occurs near both contact edges in the case of the indentation by the truncated punch specimen since it has very small R ($R/a \ll 1$) and relatively large θ (45°). While, in the case of the rounded punch specimen, it is thought that the maximum traction occurs further inward from the contact edges due to the larger radius.

By the above consideration, the findings in the experiment may be explained. In the case of partial slip, the slip region is found shorter when the truncated punch specimen is used (Fig. 5). Because the rounding radius is very small and the obliquity is comparatively large in the case of the truncated punch specimen, the traction is anticipated to have the higher peak at the location close to the contact edges compared with those by the rounded punch specimen. Since the analysis results show that the slip region cannot exceed inward from the location of maximum traction, the width of it must be small. Instead, the wear volume by the truncated punch is found greater since the work done onto the contact surface is the same for both specimens (i.e., the same shear force and displacement are applied to both specimens). It is regarded here that the amount of wear is closely related with the work done onto the contact surface. From this, it is also possible to explain that the rounded punch specimen causes the longer scar but less volume of wear.

Besides the strip specimen of the present analysis, such contact shapes can be applied to the edge machining of contacting components in the mechanical structures. So to speak, rounding and chamfering at the sharp edges are commonly used in the manufacturing process for handling safety as well as relieving the stress concentration. Present results give the guide of dimensioning them. For instance, a certain magnitude of rounding can be determined when the chamfering is tried to decrease the peak traction apparently. Present work provides the fundamental view of the partial slip solution corresponding to the rounding and chamfering. The shear force considered for the analysis is generally caused by the vibration between contacting components during service. Therefore, this work may also be used as an implementation of guideline to control the vibration amplitude of the components to restrain contact-induced failure, especially wear. Since the normal and shear tractions are obtained, the internal stress can also be readily evaluated. So it is possible to analyze the cracking failure by fracture mechanical analysis, which has been done elsewhere [12]. From these works, it is advocated here that to design the appropriate contact shape is one of the efficient methods to control the contact-induced failure.

Concluding Remarks

Considered in this research is the possibility of controlling contact-induced failure by improving the shape of the end profile (contact shape) of contacting bodies. Contact tractions of partial slip condition are investigated theoretically. The influence of the contact shape on wear is also examined experimentally. Partial slip rather than gross slip is brought into focus to restrain wear. From the obtained results, the following conclusions can be derived. Firstly, the rounding at the sharp

edges of contacting bodies decreases the peak of the contact traction considerably. In the case of rounded punch, the location of the maximum traction moves inward from the contact edges as the radius increases. While, in the case of truncated punch, the obliquity affects the location of the maximum traction. It moves inward as the obliquity decreases. The traction shape by the truncated and rounded punch (TR-punch) is influenced by both obliquity and rounding radius. So it is necessary to choose the best combination of them (i.e., the obliquity and the rounding radius) in the design stage of TR-punch-shaped components, which is widely found in the actual mechanical components. Secondly, it is found that the slip region in the partial slip regime cannot expand inward further into the central region inside the peak (maximum) tractions. If the shear force is exerted further than that, everywhere on the contact surface slides (gross slip). Since wear occurs on the slip region, the shape control of the end profile of contacting bodies is also necessary to decrease wear damage. So, it is soundly concluded that improving the contact shape can restrain the contact-induced failure. Present work may also provide an efficient tool for the design of edge machining of the contacting components.

Acknowledgment

This work has been carried out under the Nuclear R&D Program by Ministry of Science and Technology in Korea.

References

1. Tanaka, K., Mutoh, Y., Sakoda, S. and Leadbeater, G., Fretting Fatigue in 0.55C Spring Steel and 0.45C Carbon Steel, Fat. Fract. Engng Mater. Struct., Vol. 8, No. 2, pp. 129-142, 1985.
2. Troshchenko, V.T., Tsybanev, G.V. and Khotsyanovsky, A.O., Two-parameter Model of Fretting Fatigue Crack Growth, Fat. Fract. Engng Mater. Struct., Vol. 17, No. 1, pp. 15-23, 1994.
3. Hills, D. A., Nowell, D and Sackfield, A., Mechanics of Elastic Contacts, Butterworth-Heinemann Ltd., Oxford, UK, 1993.
4. Ko, P.L., The Significance of Shear and Normal Force Components on Tube Wear due to Fretting and Periodic Impacting, Wear, Vol. 106, pp. 261-281, 1985.
5. Kim, H.-K. and Kim, S.-J., Development of Algorithm for Wear Volume Evaluation using Surface Profile Analysis, J. Kor. Soc. Tribologists and Lubr. Engrs., Vol. 17, No. 1, pp. 33-39, 2001.
6. Kim, H.-K., Kim, S.-J., Yoon, K.-H., Kang, H.-S. and Song, K.-N., Fretting Wear of Laterally Supported Tube, Wear, Vol. 250, pp. 535-543, 2001.
7. Fouvry, S., Kapsa, P. Zahouani, H. and Vincent, L., Wear Analysis in Fretting of Hard Coatings through a Dissipated Energy Concept, Wear, Vol. 203-204, pp. 393-403, 1997.
8. Fouvry, S., Kapsa, P. and Vincent, L., Quantification of Fretting Damage, Wear, Vol. 200, pp. 186-205, 1996.
9. Ciavarella, M. and Demelio G., On Non-symmetrical Plane Contacts, Int. J. Mech. Sci., Vol. 41, No. 12, pp. 1533-1550, 1999.
10. Kim, H.-K., Hills, D.A. and Nowell, D., Partial Slip between Contacting Cylinders under Transverse and Axial Shear, Int. J. Mech. Sci. Vol. 42, No. 2, pp. 199-212, 2000.
11. Ciavarella, M., Hills, D.A. and Monno G., The influence of rounded edges on indentation by a flat punch, Proc. IMechE Part C, Vol. 212, pp. 319-328, 1998.
12. Kim, H.-K. and Lee, S.-B., Influence of Indenter Geometry on Half-plane with Edge Crack subjected to Fretting Condition, Theo. Appl. Fract. Mech., Vol. 36, No.2, pp. 125-139, 2001.